THE JOURNAL OF PHYSICAL CHEMISTRY C

Article

pubs.acs.org/JPCC

Micro- and Macroscopic Modeling of Sputter Depth Profiling

Dawid Maciazek,[†] Robert J. Paruch,[‡] Zbigniew Postawa,[†] and Barbara J. Garrison*[,‡]

[†]Smoluchowski Institute of Physics, Jagiellonian University, ulica Lojasiewicza 11, 30-348 Krakow, Poland

[‡]Department of Chemistry, Penn State University, 104 Chemistry Building, University Park, Pennsylvania 16802, United States

S *Supporting Information*

ABSTRACT: A model for predicting depth profiles due to energetic particle bombardment based on the RMS roughness of the system and the sputtering yield is proposed. The model is an extension of the macroscopic transport model proposed previously [Tuccitto, N.; Zappala, G.; Vitale, S.; Torrisi, A.; Licciardello, A. *J. Phys. Chem. C* **2016**, *120*, 9263−9269]. The model is used to reconstruct the experimental depth profiles of a NiCr heterostructure due to bombardment by C_{60}, SF_5, O_2, and Ga.

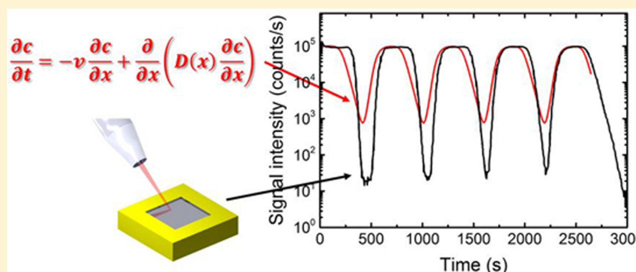

1. INTRODUCTION

Efforts have been undertaken toward understanding the factors involved in depth profiling of atomic and molecular solids due to bombardment by energetic projectiles. Typical model systems include embedded delta layers and multilayer heterostructures. The first models introduced the three fundamental factors for depth profiling, that is information depth of sputtered material, ion-beam mixing, and surface roughness.[1,2] These models propose analytic functions for fitting to experimental data and are useful in many applications. The procedure, however, of how to incorporate microscopic information on the atomic or molecular motion, such as comes from atomistic molecular dynamics (MD) simulations, is not clear.

A model has been developed recently to take information from MD simulations and predict the depth profile of a delta layer.[3−6] This model is valuable in providing insight as to how the physics from the MD simulations fits with the concepts of roughness, information depth, and mixing. The computational complexity of this model and the underlying MD simulations, however, make it prohibitive to consider large depths and long times. As a result, modeling depth profiling of systems with 100s of nm depth and inclusion of long time scale processes, such as thermal diffusion, is not tractable. It is also not clear how to connect experimental quantities with the calculated depth profile.

Recently, a continuum transport and reaction model of depth profiling due to energetic ion-beam bombardment or sputtering has been proposed by Tuccitto et al.[7] The physics associated with sputtering, specifically the sputtering yield and the ion-beam damage or displacements, are associated with the macroscopic processes of advection and diffusion, respectively. A reaction term has also been incorporated to include bombardment-induced chemistry. This transport model is capable of correctly reproducing qualitative features of a depth profile. It is not clear, however, how the parameters of this model map to the microscopic quantities of MD simulations or experimental data. On the other hand, incorporating quantities such as thermal diffusion and modeling large sample depths is straightforward and easy to compute.

We have long been proponent of analytic models that incorporate input from MD simulations, especially for the ion-beam bombardment process of secondary ion mass spectrometry (SIMS). These include the mesoscale energy deposition footprint (MEDF) model[8,9] and the steady-state statistical sputtering model (SS-SSM).[4,5] In the MEDF model, the energy deposition profile from short-time MD simulations of cluster particle bombardment are used to provide input into an analytic model to predict sputtering yields as a function of incident energy. The SS-SSM uses input from repetitive bombardment MD simulations[10] to predict the corresponding depth profile of a delta layer. For C_{60} and Au_3 bombardment of a Ag surface, it was found that the best depth profiles resulted when the sputtering yield was high relative to the amount of ion-beam mixing or damage.[5]

In this study, we propose how to use the SS-SSM and underlying MD simulations to determine how to interpret and choose input into the transport model. Specifically we will use the examples of C_{60} and Au_3 bombardment of Ag(111)[4,5] and C_{60} bombardment of a molecular solid of octane.[6] On the basis of this development, we propose simple relationships of the input quantities to the transport model based on only the experimental quantities of sputtering yield and RMS roughness. The predicted depth profiles from these parametrizations will be compared to the depth profiles predicted by the SS-SSM. Finally, we predict depth profiles for C_{60}^+, Ga^+, SF_5^+, and O_2^+ depth profiling of a NiCr heterostructure and explain the beam type dependence of the experimental depth profiles.[11−13] The

Received: September 12, 2016
Revised: October 12, 2016
Published: October 19, 2016

 © 2016 American Chemical Society

DOI: 10.1021/acs.jpcc.6b09228
J. Phys. Chem. C 2016, 120, 25473−25480

ultimate target to be addressed in future studies is explaining the temperature dependence of depth profiling of Irganox delta layers.[14−16] The ability to incorporate the experimental data directly into the transport model makes this model useful in direct interpretation of experimental results.

2. MICRO- AND MACROSCOPIC DESCRIPTIONS OF SPUTTER DEPTH PROFILING

The first step is to establish a procedure for using the results of the repetitive bombardment MD simulations and the SS-SSM analysis to understand and quantify the input quantities of the transport model in terms of the basic physics and motion of the bombardment process. On the basis of this analysis and comparison, we formulate an empirical approach based on only experimental quantities for determining the input quantities of the transport model.

2.1. Transport and Reaction Model. This model is described in detail in the original reference[7] and is based on the advection−diffusion−reaction equation for mass transfer

$$\frac{\partial c}{\partial t} = -v\frac{\partial c}{\partial x} + \frac{\partial}{\partial x}\left(D(x)\frac{\partial c}{\partial x}\right) + R(x) \tag{1}$$

The independent variables are t = time [s] and x = depth [nm]. The dependent variable is $c = c(x;t)$ = concentration profile of mass (or number of atoms/molecules). The parameters are v = velocity the mass is traveling with [nm/s], $D(x)$ = depth dependent diffusivity [nm^2/s], and $R(x)$ = depth dependent reaction term [1/s], a quantity not utilized in this study. The initial condition is $c_0 = c(x;t=0)$. A second equation of the same form, with its own set of the parameters, can be added to model the depth profiling of the second component as is needed for the NiCr heterostructure. The initial concentration profile of a delta layer is modeled as a double sigmoid. It corresponds to a layer of mass embedded in the sample at given depth. As the time passes, the mass travels toward the surface of the sample, $x = 0$. During this process the profile changes its shape due to the effect of $D(x)$. In the original model, the depth profile is determined only by the concentration of the delta layer component at the surface as time is progressed in the numerical integration.[7] Below we will propose a method to include information depth in the transport model based on MD simulation results.

2.2. Information Available in MD Simulations and the SS-SSM. The first step is to assess the information available in the MD simulations and the SS-SSM[4−6] analysis to make a connection to the transport model. The critical quantities that arise in a straightforward analysis from the repetitive bombardment MD simulations[10] are the yield expressed in volume per impact and the RMS roughness. The SS-SSM[4−6] provides a formalism for analyzing the results of the MD simulation and also predicts depth profiles of delta layers. The SS-SSM divides the MD system into layers and calculates quantities on a per layer basis. The surface is roughened thus all quantities are relative to the average surface level. The three quantities of relevance are the sputtering yield per layer, displacements of atoms or molecules from one layer to another, and the average occupation of each layer.

The sputtering, displacement, and occupancy distributions as determined in the SS-SSM from the MD simulations are for a roughened surface, whereas the transport model assumes a flat surface. The first step in making these two approaches compatible is to ignore the information from the volume above the average surface level, peaks in the roughened surface, as there are relatively few particles here. Second, the distributions from the average surface level (50% occupancy) and into the substrate are normalized by the occupancy of each layer. Thus, the distributions now appear as they are from a flat surface. The roughness information remains, however, in the widths of the distributions. In addition, the displacement distributions in the SS-SSM were for movement up and down. These have been converted to movement by one layer, by two layers, and by three layers, where each of these quantities is known as a function of layer position. Finally, the number of atoms per layer that do not move vertically are determined. This step is essential for determination of the value of the ion-beam mixing term. Of note is that for each layer the sum of the number of atoms that do not move, that move one layer, that move two layers, etc., is approximately proportional to the surface area of the master sample used in the MD simulation. Later, we will use the explicit surface area of the master sample for the calculation of time between impacts, and it is important to realize that this information will cancel out.

2.2.1. Velocity. The velocity v that the mass is traveling with is the rate at which the surface recedes and is associated with the sputtering yield, Y, in nm^3 and experimental fluence, F, in ions/(nm^2 s) as

$$v = FY \tag{2}$$

2.2.2. Sampling Depth. In the original formulation,[7] the depth profile is determined only by the concentration of the delta-layer component as it approaches the surface. In reality, however, also particles located below the surface are being ejected by a single projectile impact. The depth distribution of a number of atoms ejected by a single impact is known as a sampling or information depth. This quantity can be easily determined from the sputtering distributions given by the MD simulations. We normalize this function to a unit area as the total sputtering yield is incorporated in the velocity. The normalized sampling depth, $S(x)$, is subsequently used as a weighting factor for the concentration profile, $c(x)$, to calculate ejected mass in the predicted depth profile. In addition to containing information about the depth of origin of the sputtered particles, it implicitly contains information about the RMS roughness.

2.2.3. Ion-Beam Mixing and Diffusion. The ion-beam mixing and diffusion has the form of

$$D_{total} = D(x) + D_{diff} \tag{3}$$

where $D(x)$ is the depth-dependent ion-beam mixing term. True thermal diffusion is represented by D_{diff} and is a constant component that can be temperature dependent.

Conceptually, there is a challenge to tie ion-beam mixing to diffusion. Diffusion is generally considered to be a long time process whereas the ion-beam mixing occurs on a time scale up to tens of picoseconds. Even by examining MD simulations, providing a precise time scale is challenging. We start, however, by implementing the formula used for calculating a diffusion constant in MD simulations. Diffusivity for an infinite one-directional system is described as

$$D(x) = \frac{1}{2}\lim_{t\to\infty}\frac{\langle \mathrm{disp}(x)^2\rangle}{t} \tag{4}$$

The sputtering process and associated ion-beam mixing do not exactly fit with the above description, but in order to find a

DOI: 10.1021/acs.jpcc.6b09228
J. Phys. Chem. C 2016, 120, 25473−25480

connection between the macroscopic model for depth profiling and the microscopic motions we assume a similar relation as

$$D(x) = \frac{1}{2}\frac{\langle \mathrm{disp}(x)^2\rangle}{\Delta t} \quad (5)$$

where Δt is a time interval and thus we proceed from here. To calculate the quantity $\langle \mathrm{disp}(x)^2\rangle$, we use the information contained in the displacement distributions from the SS-SSM analysis as described above modified to account for the flat surface. For each depth we calculate the number of atoms that are displaced by one layer, by two layers, three layers, etc., and the number of atoms that are not displaced. The displacement term is thus a sum of the number of atoms that are displaced one layer times the layer spacing squared plus the number of atoms displaced two layers times twice the layer spacing squared, etc., divided by the total number of atoms. As noted above, the total number of atoms per layer is approximately proportional to the area of the master sample used in the MD simulations. The quantity Δt is assumed to be the time between impacts on the master sample or the reciprocal of the area of the master sample times the fluence F. The final situation is that we have used the SS-SSM displacement distributions to calculate a $D(x)$ value. The time factor has an area of the master sample which effectively cancels out the total number of atoms in a layer in the MD simulation, a factor that is not physically relevant. Overall, then we can write $D(x)$ as

$$D(x) = FD'(x) \quad (6)$$

where $D'(x)$ has units of nm^4 per impact. This quantity $D'(x)$ does not depend on the fluence, the time between impacts, or the size of the master sample. It is a quantity related to an average over single impacts much like the sputtering yield is an average over individual impact events. Now the ion-beam mixing term in the macroscopic transport equation has a microscopic quantity associated with it. At this point we are not prepared to make a precise physical interpretation of the $D'(x)$ term. What is clear, however, is that $D'(x)$ only depends upon properties associated with the individual impact events and not any long time diffusion-like behavior. This quantity should depend upon the projectile beam type, the incident kinetic energy, KE, of the projectile beam, and the material properties including displacement energies. Following the convention that sputtering yields[17] are proportional to the ratio of the KE to the cohesive energy, U_0, we assume the integral of $D'(x)$ over depth to be proportional to KE/U_0 when we discuss below the application of the transport model to the experimental NiCr heterostructures.

To summarize, we used the displacement distributions from the MD simulations and the SS-SSM analysis to define a microscopic ion-beam mixing diffusion term, $D(x)$. This relation results in the ion-beam mixing term to be a product of the fluence times a term that corresponds a quantity, $D'(x)$, related to single impacts.

For convenience, we assume the fluence to be 1 ion/(nm^2 s) which corresponds to an ion current density of 6.4 nA per (200 μm)^2. These conditions are in the experimental regime for C_{60} cluster sources. In fact, if there is no time-dependent quantity such as diffusion in the transport equation, the fluence does not matter in this model or in the experiment if the depth profile is shown as a function of depth rather than time. For comparisons with experimental data shown below, the apparent fluences are taken from the experimental data.

2.2.4. Verification of the Transport Model Depth Profiles vs the SS-SSM Depth Profiles. The first step is to define the $S(x)$ and $D'(x)$ quantities from the MD simulations and the SS-SSM quantities, incorporate them into the transport model, and compare the depth profiles. Repetitive bombardment MD simulations have been performed for three systems and the results analyzed by the SS-SSM with the results presented in previous publications.

- 20 keV C_{60}/Ag(111).[4−6,18] The sputtering yield is 6.4 nm^3 (or 373 atoms) per impact,[6] and the RMS roughness of the system is 2.35 nm.[5]
- 20 keV Au_3/Ag(111).[5,18] The sputtering yield is 3.69 nm^3 (or 216 atoms) per impact, and the RMS roughness of the system is 2.69 nm.
- 10 keV C_{60}/octane.[6] The total sputtering yield is 147 nm^3 (or the equivalent of 703 molecules),[6] and the RMS roughness is 3.3 nm.

Only the yields and RMS values are given explicitly here as these are the quantities most directly comparable to information that can be extracted in experiments.

As the differential equation solver that we use requires an analytical form of the input distributions sigmoidal functions are fit to the sampling depth distributions, $S(x)$, as well as the ion-beam mixing terms, $D'(x)$, obtained from the SS-SSM model. The results are shown in Figure 1 with the sigmoid function equation given in the Supporting Information and the parameters given in Table 1.

The sampling distributions $S(x)$ shown in Figure 1a are normalized to unit area since they are weighting functions used to obtain sputtered signal from concentration profiles. The distributions for the three systems are similar to basically the

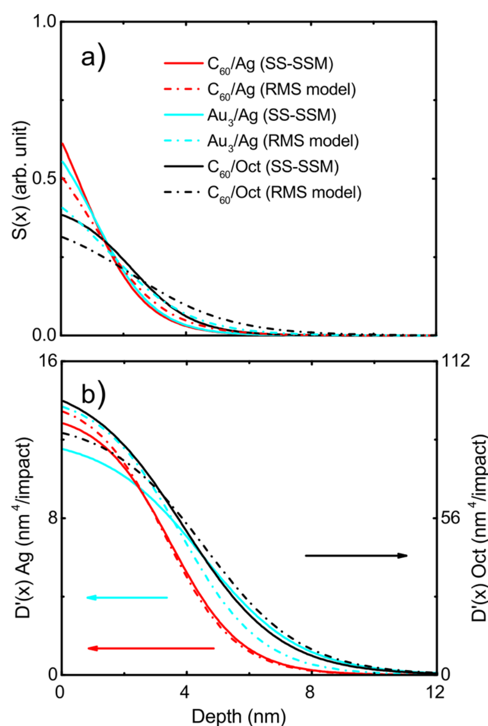

Figure 1. Distributions for use in the transport model for the three systems. (a) Sampling depth, $S(x)$, from SS-SSM values and the RMS model. (b) Ion-beam mixing, $D'(x)$, from SS-SSM values and RMS model; right-hand side scale is for octane, and left-hand side scale is for Ag.

DOI: 10.1021/acs.jpcc.6b09228
J. Phys. Chem. C 2016, 120, 25473−25480

Table 1. Parameters for the Transport Model Based on the MD Results and SS-SSM Analysis

		sampling depth, $S(x)$			ion-beam mixing, $D'(x)$		
	velocity (nm/s)	amplitude	slope (1/nm)	inflection (nm)	amplitude (nm^4/impact)	slope (1/nm)	inflection (nm)
20 keV C_{60}/Ag(111)	6.4	0.94	1.02	0.66	13.5	0.88	3.48
20 keV Au_3/Ag(111)	3.7	0.74	1.05	1.09	12.2	0.64	4.50
10 keV C_{60}/octane	147	0.42	1.03	2.28	105.8	0.65	3.90

entire curve at distances less than the twice the RMS roughness. The ion-beam mixing, $D'(x)$, functions are shown in Figure 1b. The ion-beam mixing curves are broader than the sampling distributions, consistent with the information from the MD simulations and SS-SSM analysis which shows that the ion-beam mixing occurs at a deeper depth than the sputtering process. The ion-beam mixing distributions are similar in magnitude for C_{60} and Au_3 bombardment of Ag and a factor of 7 larger for C_{60} bombardment of octane. Explaining the large difference is beyond the scope of this study as we need to develop a better physical or computational picture of $D'(x)$. Even though the RMS roughness is not explicitly included in the model, information about the RMS roughness does implicitly appear in the distributions in Figure 1.

The depth profiles calculated with the SS-SSM, which were interpreted previously,[5,6] are shown in Figure 2a. In the transport model, the delta layer is represented by a double sigmoid as described in the Supporting Information. The depth profiles calculated by the transport model using input from the MD results with SS-SSM analysis are shown in Figure 2b. The SS-SSM distributions do not have an associated time scale; thus, the transport model distributions are shown as a function of depth with the velocity being the conversion factor. In our opinion, there is qualitative agreement between the depth profiles predicted by the transport model and those from the SS-SSM. The worst agreement is for the octane system in which the leading edge of the depth profile from the transport equation is too narrow. In examining the SS-SSM sputtering distribution for this system,[6] it is apparent that a significant amount of material is ejected from above the average surface level, and the assumption stated earlier that we can ignore the peaks of the roughened surface is not valid.

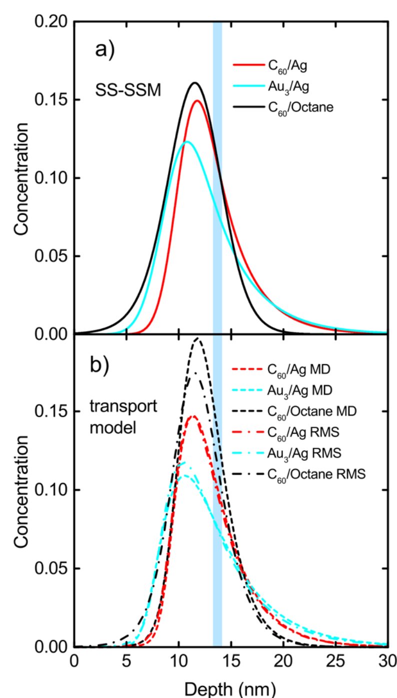

Figure 2. Depth profiles for a delta layer, represented by the blue vertical bar, of thickness 1 nm at a depth of 13.2 nm in the solid: (a) SS-SSM; (b) transport model with input from MD results and from the RMS model.

2.2.5. Development of an Empirical RMS Model. We feel that we have shown the correspondence between the terms in the transport equation and the microscopic quantities of the MD simulations. Our approach of using information from repetitive bombardment MD simulations provides the quantitative link and the conceptual definition of the impact related ion-beam mixing term, $D'(x)$. This approach, however, is not practical for use with experimental data. Consequently, using insights from the previous calibration studies, we developed a simple model that uses the RMS roughness value and the sputtering yield, both quantities that are available from MD simulations or experimental data. This model, called the RMS model for input to the transport equation, is based on following assumptions.

- The inflection point in the $D'(x)$ distribution is proportional to the RMS value.
- The inflection point in the $S(x)$ distribution is smaller than D' inflection point by a constant value, d, since the analyses of the MD results by the SS-SSM show this to be the case for the model systems.
- The area under the curve of $D'(x)$ is given, for now, by the area under the curve from the MD results. This assumption is the main area needed for improvement of the RMS model and, in fact, understanding the basic physics underlying $D'(x)$.
- For each the $S(x)$ and $D'(x)$ sigmoid functions, ignoring the amplitude, we assume that 90% of the amplitude change of the function is between distances of zero and twice the inflection point, a distance denoted "cut". Since the sigmoid function is antisymmetric around the

Table 2. Parameters for the Transport Model Based on the RMS Model

		sampling depth, $S(x)$			ion-beam mixing, $D'(x)$		
	velocity (nm/s)	amplitude	slope (1/nm)	inflection (nm)	amplitude (nm^4/impact)	slope (1/nm)	inflection (nm)
20 keV C_{60}/Ag(111)	6.4	0.72	0.89	1.01	13.46	0.89	3.31
20 keV Au_3/Ag(111)	3.7	0.54	0.77	1.50	12.18	0.77	3.81
10 keV C_{60}/Octane	147	0.39	0.64	2.28	105.8	0.64	4.58

DOI: 10.1021/acs.jpcc.6b09228
J. Phys. Chem. C 2016, 120, 25473−25480

Table 3. Experimental Conditions

	RMS (nm)	velocity (nm/s)	Y (nm^3)	sampling depth amplitude	sampling depth slope (1/nm)	sampling depth inflection (nm)	$D'(x)$ amplitude (nm^4/impact)	$D'(x)$ slope (1/nm)	$D'(x)$ inflection (nm)
15 keV C_{60}^+/NiCr	2.5	0.0518	2.95	0.628	0.835	1.23	6.78	0.835	3.53
15 keV Ga^+/NiCr	100	0.0122	0.174	0.007 07	0.0209	138.7	0.2	0.0209	141
3 keV SF_5^+/NiCr	10	0.201	0.174	0.082	0.209	11.8	0.181	0.209	14.1
3 keV O_2^+/NiCr	62	0.441	0.087	0.011	0.0337	85.1	0.0644	0.0337	87.4

inflection point, this means that at a distance of twice the inflection point the value of the function should be 0.05 and the value at zero should be 0.95. This allows us to determine the slope to be

$$\text{slope} = \frac{\ln(1/\text{cut}^{-1})}{\text{inflection point}} \tag{7}$$

We have found that a good agreement between the depth profiles predicted by this simplified RMS model and the depth profiles using MD input can be obtained, if the inflection point for $D'(x) = 1.4 \cdot \text{RMS}$ and $d = 3.2$ nm as shown in Figure 2b. The calculated sigmoid function parameters of the RMS model for the three systems are given in Table 2, and the $S(x)$ and $D'(x)$ distributions are shown in Figure 1. Regardless of its simplicity, the RMS model reproduces the depth profiles of the SS-SSM method as well as the functions based on the MD results. We have, of course, used information from the MD results to give the area under the $D'(x)$ curve for the RMS model.

The effect of thermal diffusion on the Ag depth profiles can be easily tested in the transport model by setting the D_{diff} parameter. For Ag, self-diffusion has been measured over the temperature ranges of 454−777 K[19] and 903−1208 K,[20] and temperature-dependent diffusion constants have been determined. If these relations are extrapolated to 300 K, the diffusion constant is on the order of 10^{-18} nm^2/s. This value can be added to the calculation, but this value is 18 orders of magnitude smaller than the ion-beam mixing values; thus, it is obvious that no significant thermal diffusion occurs in Ag. The big point, however, is that both ion-beam mixing and thermal diffusion can be accommodated within the transport model.

3. INTERPRETATION OF EXPERIMENTAL DATA

We now take the RMS model one step further and try to reproduce experimental depth profiles of NiCr heterostructures. It will be an important test of model versatility as these depth profiles were obtained with four very different beam conditions. The NiCr heterostructure sample has nine alternating layers of Cr and Ni with the five Cr layers 53 nm thick and the four Ni layers 66 nm thick for a total depth of 529 nm. Two groups have performed depth profiling experiments on this standardized sample. First, Gillen et al. have used 3 keV SF_5^+ and O_2^+ beams and measured the Ni^+ and Cr^+ signals.[13] Second, Sun et al. have performed experiments using 15 keV C_{60}^+ and Ga^+ beams and measured the Ni and Cr signals with multiphoton resonance ionization.[11,12]

The objective of this analysis is to use the available experimental data to predict the depth profiles using the transport model using the RMS model to generate input functions. The three main quantities in the model are the sputtering yield, the displacement quantity $D'(x)$, and the fluence. The quantities that appear in the experiment are the time to depth profile through the 529 nm of material, the RMS roughness, and the sputtering yields for the C_{60}^+ and Ga^+ beams. The experimental time to depth profile through the sample was used to calculate the average velocity in the model. The obtained values are given in Table 3. In the original publications,[11,12] for C_{60}^+ and Ga^+ bombardment, the yields were given in atoms per impact, and we converted these to nm^3 by assuming the single crystal atomic density. For Ni and Cr both the atomic densities and yield are within 9% of each other so we used the averaged values for these quantities. The effective fluence is the velocity divided by the yield. This value accounts for the fluence of the beam and also the effect of rastering the beam to produce a depth profile.

The yields for SF_5^+ and O_2^+ bombardment were determined by simulation using the experimental values for C_{60}^+ and Ga^+ as reference points. The calculation of absolute sputtering yields is challenging because none of the interaction potentials are completely accurate and because some physics is missing such as energy loss to electronic effects. Thus, our strategy is to use comparable simulations to estimate relative yields and then determine an estimate of the experimental yields for SF_5^+ and O_2^+ bombardment based on the experimental C_{60}^+ and Ga^+ yields. Previously we determined from MD simulations the yields for C_{60} and Ga bombardment of Ag at 15 keV to be 331 and 21 atoms per impact.[21] No potentials exist for bombardment of SF_5 and O_2 on Ag, and we do not want to include too much potential variation so we tried to construct hydrocarbon analogues for these two projectiles. We chose projectiles of neopentane $C(CH_3)_4$ and C_2 (with mass of O rather than C). One hundred impacts were calculated for each projectile on the flat surface at an energy of 3 keV and the experimental impact angle of 52°. The calculated yields are 21.6 ± 1.5 and 10.2 ± 1.0 atoms/impact for $C(CH_3)_4$ and C_2, respectively. The neopentane calculated yield is almost the same as the Ga calculated yield, and the C_2 yield is about half the Ga calculated yield on Ag; thus, we scale the experimental yields for Ga^+ on NiCr for SF_5^+ and O_2^+ as given in Table 3. The effective fluence is calculated from the experimental average velocity.

The RMS model is used with the experimental RMS values to determine the $S(x)$ and $D'(x)$ functions as shown in Figure 3. For the area under the $D'(x)$ curve we feel that the appropriate calculation should be for the metal substrate, and since $D'(x)$ for both the C_{60} and Au_3 projectiles have similar areas, we chose the 20 keV Au_3/Ag system, which has a value of 55.8 nm^5. This value was scaled for each set of beam conditions by KE/U_0, as it is commonly used to scale sputtering yields.[22] We assume that it is also a logical scaling factor for displacements. The value of U_0 for Ag is 2.93 eV,[23] and the average value for the NiCr system is 4.27 eV.[23] The four experimental conditions break into two groups depending on the RMS value. The RMS values for the C_{60}^+ and SF_5^+ bombardment are 2.5 and 10 nm, respectively. For these two systems the axes at the left and bottom of Figure 3 should be

DOI: 10.1021/acs.jpcc.6b09228
J. Phys. Chem. C 2016, 120, 25473−25480

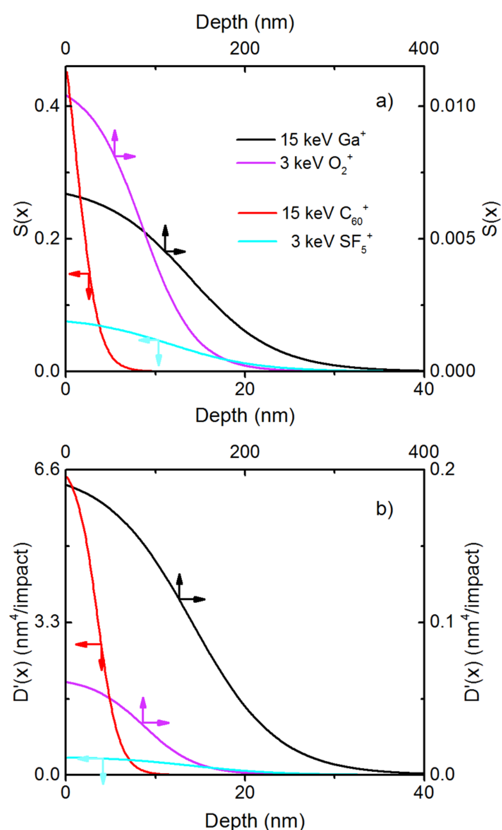

Figure 3. $S(x)$ and $D'(x)$ functions for the NiCr system for the four beam conditions using the RMS model.

used. The $S(x)$ and $D'(x)$ functions are relatively short-ranged and intense. In contrast, the RMS values for O_2^+ and Ga^+ have larger RMS values of 62 and 100 nm, respectively. The right and top axes should be used for their $S(x)$ and $D'(x)$ functions. These functions are longer-ranged and less intense than the ones for C_{60}^+ and SF_5^+. Of note is that the NiCr layers are 53 and 66 nm wide, distances larger than the C_{60}^+ and SF_5^+ functions, smaller than the Ga^+ functions, and comparable to the O_2^+ functions.

The predicted depth profiles are shown in Figure 4 overlaid on the experimental data that was digitized from the original literature. The double sigmoid used to describe the NiCr heterostructure is described in the Supporting Information. We have maintained the plot representation, linear vs log scale, of the experimental publications. The intensities of the individual Ni and Cr signals have a multitude of experimental factors so we used two normalization factors per plot. Overall, we are pleased with the agreement between the transport model depth profiles using the RMS model for predicting the $S(x)$ and $D'(x)$ functions with the experimental data. The RMS roughness values for C_{60}^+ and SF_5^+ bombardment are less than the heterostructure layers, and consequently the depth profiles show discrete layers. For the O_2^+ and Ga^+ bombardment there is an induction time to develop the large RMS roughness values, a factor not included in the transport model. Even with this omission, we feel that the predicted depth profiles qualitatively reproduce the experimental distributions. We did try not using KE/U_0 to scale the $D'(x)$ area. The resulting depth profiles were slightly broader but not qualitatively different.

There is one additional piece of information available in the experimental study on the C_{60}^+ bombardment of NiCr;[11]

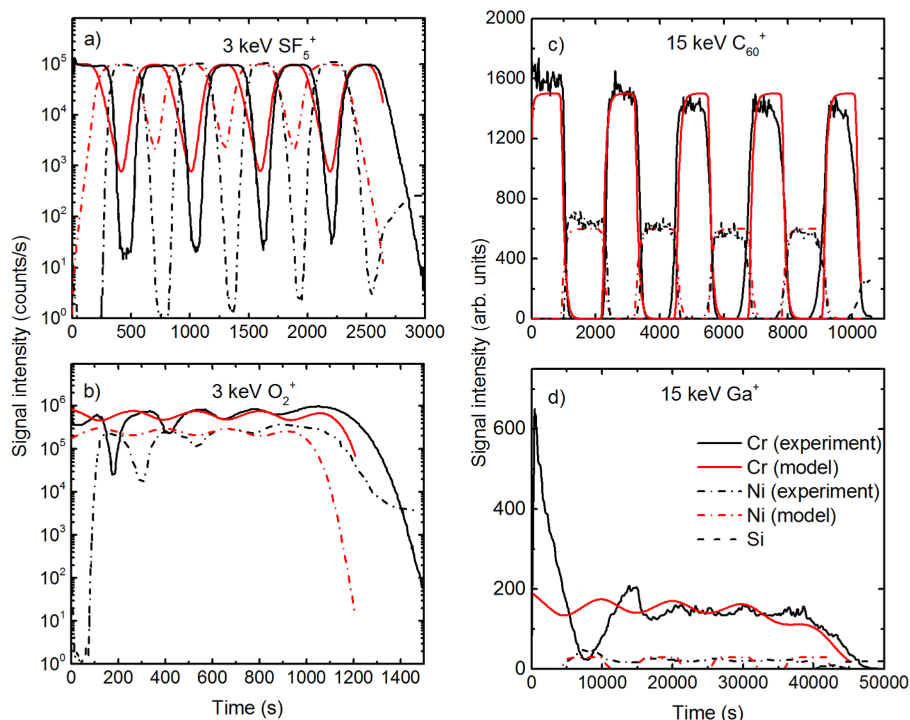

Figure 4. Dependence of signals of ions (a, b) and neutral atoms (c, d) on the sputter time for a nine-layer Ni:Cr multilayer stack bombarded by (a) 3 keV SF_5^+, (b) 3 keV O_2^+, (c) 15 keV C_{60}^+, and (d) 15 keV Ga^+. Black curves depict experimental signal of Cr (solid line) and Ni (dash-dotted line) atoms, while red curves depict analogous data obtained from the RMS model. The dashed black line depicts experimental intensity of the substrate Si signal which was not modeled.

DOI: 10.1021/acs.jpcc.6b09228
J. Phys. Chem. C 2016, 120, 25473−25480

namely, the intensity of the NiCr dimer is measured as a function of time. The emission of these dimers should only occur where both Ni and Cr are present in the sample, that is, at the interfaces between the layers. The experimental data clearly show that the widths of the NiCr peaks increase as the material is depth profiled. This observation is also slightly visible in the experimental depth profile shown in Figure 4c. The transport model does not show the same broadening, and in fact, it cannot since the $S(x)$ and $D'(x)$ functions become vanishingly small at about one-half the layer width. This discrepancy implies to us that some experimental condition may not be fully controlled or understood. One possibility could be, for instance, nonuniform material removal, which would result in a formation of a crater with a bottom that becomes less parallel to the sample surface with time.

4. CONCLUSIONS

Using results from molecular dynamics simulations and the steady-state statistical sputtering model for predicting depth profiles due to energetic particle bombardment, we have defined the quantities in a macroscopic model for predicting depth profiles based on the transport equation. Specifically, we developed a microscopic definition for the ion-beam mixing or diffusion term, a quantity that is associated with the amount of displacements in the individual impact event. In addition, we proposed a protocol to incorporate sampling or information depth calculated from individual impacts, a term that was not present in the original model. The transport model for depth profiling was calibrated for three test cases for which there are associated repetitive bombardment MD simulations and predicted depth profiles from the SS-SSM. Using the functions developed for these calibration studies, we developed a simple RMS model that predicts the functions for the transport model from just the RMS roughness value and the sputtering yield. We show that we can reproduce the depth profiles of a NiCr heterostructure for four beam conditions that range from RMS values of 2.5 to 100 nm. In addition, we interpret the observed broadening of the depth profile for C_{60} bombardment, the system with the smallest RMS value of 2.5 nm, to be due to some unknown experimental condition. The main open issue is how to define theoretically the impact related ion-beam mixing term and develop a protocol for calculating it.

■ ASSOCIATED CONTENT

Supporting Information

The Supporting Information is available free of charge on the ACS Publications website at DOI: 10.1021/acs.jpcc.6b09228.

Procedure used to solve eq 1; definition of sigmoid functions used in our study (PDF)

■ AUTHOR INFORMATION

Corresponding Author

*E-mail bjg@psu.edu.

Notes

The authors declare no competing financial interest.

■ ACKNOWLEDGMENTS

The authors gratefully acknowledge the financial support from the National Science Foundation, Grant CHE-1212645, and the Polish National Science Center, Program 2013/09/B/ST4/00094.

■ REFERENCES

(1) Hofmann, S. Atomic Mixing, Surface Roughness and Information Depth in High-Resolution AES Depth Profiling of a GaAs/AlAs Superlattice Structure. *Surf. Interface Anal.* **1994**, *21*, 673−8.

(2) Dowsett, M. G.; Rowlands, G.; Allen, P. N.; Barlow, R. D. Analytic Form for the SIMS Response Function Measured from Ultra-Thin Impurity Layers. *Surf. Interface Anal.* **1994**, *21*, 310−315.

(3) Krantzman, K. D.; Wucher, A. Fluence Effects in C_{60} Cluster Bombardment of Silicon. *J. Phys. Chem. C* **2010**, *114*, 5480−5490.

(4) Paruch, R. J.; Postawa, Z.; Wucher, A.; Garrison, B. J. Steady-State Statistical Sputtering Model for Extracting Depth Profiles from Molecular Dynamics Simulations of Dynamic SIMS. *J. Phys. Chem. C* **2012**, *116*, 1042−1051.

(5) Paruch, R. J.; Garrison, B. J.; Postawa, Z. Partnering Analytic Models and Dynamic Secondary Ion Mass Spectrometry Simulations to Interpret Depth Profiles Due to Kiloelectronvolt Cluster Bombardment. *Anal. Chem.* **2012**, *84*, 3010−6.

(6) Paruch, R. J.; Garrison, B. J.; Postawa, Z. Computed Molecular Depth Profile for C_{60} Bombardment of a Molecular Solid. *Anal. Chem.* **2013**, *85*, 11628−11633.

(7) Tuccitto, N.; Zappala, G.; Vitale, S.; Torrisi, A.; Licciardello, A. A Transport and Reaction Model for Simulating Cluster Secondary Ion Mass Spectrometry Depth Profiles of Organic Solids. *J. Phys. Chem. C* **2016**, *120*, 9263−9269.

(8) Russo, M. F.; Szakal, C.; Kozole, J.; Winograd, N.; Garrison, B. J. Sputtering Yields for C_{60} and Au_3 Bombardment of Water Ice as a Function of Incident Kinetic Energy. *Anal. Chem.* **2007**, *79*, 4493−4498.

(9) Russo, M. F.; Garrison, B. J. Mesoscale Energy Deposition Footprint Model for Kiloelectronvolt Cluster Bombardment of Solids. *Anal. Chem.* **2006**, *78*, 7206−7210.

(10) Russo, M. F., Jr.; Postawa, Z.; Garrison, B. J. A Computational Investigation of C_{60} Depth Profiling of Ag: Molecular Dynamics of Multiple Impact Events. *J. Phys. Chem. C* **2009**, *113*, 3270−3276.

(11) Sun, S.; Wucher, A.; Szakal, C.; Winograd, N. Depth Profiling of Polycrystalline Multilayers Using a Buckminsterfullerene Projectile. *Appl. Phys. Lett.* **2004**, *84*, 5177−9.

(12) Sun, S.; Szakal, C.; Roll, T.; Mazarov, P.; Wucher, A.; Winograd, N. Use of C_{60} Cluster Projectiles for Sputter Depth Profiling of Polycrystalline Metals. *Surf. Interface Anal.* **2004**, *36*, 1367−72.

(13) Gillen, G.; Walker, M.; Thompson, P.; Bennett, J. Use of an SF_5^+ Polyatomic Primary Ion Beam for Ultrashallow Depth Profiling on an Ion Microscope Secondary Ion Mass Spectroscopy Instrument. *J. Vac. Sci. Technol., B: Microelectron. Process. Phenom.* **2000**, *18*, 503−508.

(14) Mao, D.; Wucher, A.; Brenes, D. A.; Lu, C. Y.; Winograd, N. Cluster Secondary Ion Mass Spectrometry and the Temperature Dependence of Molecular Depth Profiles. *Anal. Chem.* **2012**, *84*, 3981−3989.

(15) Mao, D.; Lu, C.; Winograd, N.; Wucher, A. Molecular Depth Profiling by Wedged Crater Beveling. *Anal. Chem.* **2011**, *83*, 6410−6417.

(16) Shard, A. G.; et al. Argon Cluster Ion Beams for Organic Depth Profiling: Results from a VAMAS Interlaboratory Study. *Anal. Chem.* **2012**, *84*, 7865−7873.

(17) Nastasi, M.; Mayer, J.; Hirvonen, J. K. *Ion-Solid Interactions: Fundamentals and Applications*; Cambridge University Press: Cambridge, 1996; p 145.

(18) Paruch, R.; Rzeznik, L.; Russo, M. F.; Garrison, B. J.; Postawa, Z. Molecular Dynamics Study of the Effect of Surface Topography on Sputtering Induced by 20 keV Au_3 and C_{60} Clusters. *J. Phys. Chem. C* **2010**, *114*, 5532−5539.

(19) Lam, N. Q.; Rothman, S. J.; Mehrer, H.; Nowicki, L. J. Self-Diffusion in Silver at Low-Temperatures. *Phys. Status Solidi B* **1973**, *57*, 225−236.

(20) Tomizuka, C. T.; Sonder, E. Self-Diffusion in Silver. *Phys. Rev.* **1956**, *103*, 1182−1184.

(21) Postawa, Z.; Czerwinski, B.; Szewczyk, M.; Smiley, E. J.; Winograd, N.; Garrison, B. J. Enhancement of Sputtering Yields Due

to C_{60} Versus Ga Bombardment of Ag{111} as Explored by Molecular Dynamics Simulations. *Anal. Chem.* **2003**, *75*, 4402−4407.
(22) Paruch, R. J.; Postawa, Z.; Garrison, B. J. Seduction of Finding Universality in Sputtering Yields Due to Cluster Bombardment of Solids. *Acc. Chem. Res.* **2015**, *48*, 2529−36.
(23) Kittel, C. *Introduction to Solid State Physics*, 8th ed.; John Wiley & Sons, Inc.: Hoboken, NJ, 2005; p 50.

DOI: 10.1021/acs.jpcc.6b09228
J. Phys. Chem. C 2016, 120, 25473−25480